Impact of Diurnal Variation in Vegetation Water Content on Radar Backscatter From Maize During Water Stress

Tim van Emmerik, *Student Member, IEEE*, Susan C. Steele-Dunne, Jasmeet Judge, *Senior Member, IEEE*, and Nick van de Giesen

***Abstract*—Microwave backscatter from vegetated surfaces is influenced by vegetation structure and vegetation water content (VWC), which varies with meteorological conditions and moisture in the root zone. Radar backscatter observations are used for many vegetation and soil moisture monitoring applications under the assumption that VWC is constant on short timescales. This research aims to understand how backscatter over agricultural canopies changes in response to diurnal differences in VWC due to water stress. A standard water-cloud model and a two-layer water-cloud model for maize were used to simulate the influence of the observed variations in bulk/leaf/stalk VWC and soil moisture on the various contributions to total backscatter at a range of frequencies, polarizations, and incidence angles. The bulk VWC and leaf VWC were found to change up to 30% and 40%, respectively, on a diurnal basis during water stress and may have a significant effect on radar backscatter. Total backscatter time series are presented to illustrate the simulated diurnal difference in backscatter for different radar frequencies, polarizations, and incidence angles. Results show that backscatter is very sensitive to variations in VWC during water stress, particularly at large incidence angles and higher frequencies. The diurnal variation in total backscatter was dominated by variations in leaf water content, with simulated diurnal differences of up to 4 dB in X- through K_u-bands (8.6–35 GHz). This study highlights a potential source of error in current vegetation and soil monitoring applications and provides insights into the potential use for radar to detect variations in VWC due to water stress.**

***Index Terms*—Agriculture, diurnal differences, hydrology, microwaves, radar, vegetation, vegetation water content (VWC), water stress.**

I. Introduction

THE influence of vegetation on radar backscatter is significant in many applications, including soil moisture retrieval, [1]–[6], crop classification [7]–[10], biomass [11], [12], and forest monitoring [13], [14]. Radar observations of the land surface are sensitive to vegetation because its presence results in the two-way attenuation of the reflection signal from the soil surface, and the vegetation contributes to total backscatter by surface and volume scattering from the canopy itself [6], [11], [12]. Understanding the influence of diurnal vegetation water content (VWC) dynamics in response to water stress on radar backscatter could improve soil moisture retrievals, using microwave remote sensing, and provide insights into the potential use for radar to directly monitor vegetation water status.

Radar is used for many vegetation and soil moisture monitoring applications. In algorithms for crop classification [7]–[10] and biomass monitoring for carbon studies [13], [14], only a few radar images are used over time. Based on the assumption that VWC mainly changes on a seasonal scale [15], diurnal variations in VWC are often neglected. The water content of soil and vegetation varies diurnally and seasonally [16]. Depending on the timescale of interest, these variations could have a significant impact on radar backscatter. In cases where one is interested in seasonal changes in VWC, diurnal differences might be less important. However, Chambers *et al.* [13] stated that current hypertemporal remote sensing observations already changed our understanding of canopy VWC and phenology in tropical forests, suggesting that also for applications based on radar with longer revisit times a better understanding of diurnal differences in VWC may improve current retrieval algorithms. When studying soil and vegetation water status dynamics on a daily timescale, diurnal variations might be significant. Soil moisture retrieval algorithms for radar missions require an estimate of VWC, which is generally considered constant or to change only on a seasonal timescale [17]–[21]. In the latter case, seasonal variation is assumed to be due to canopy growth rather than diurnal moisture dynamics. Diurnal differences in VWC can thus introduce an error in soil moisture retrieval algorithms. For applications such as estimating the fuel load of vegetation [14], where foliage water content is significant [13], accounting for diurnal variation in VWC might improve vegetation fire threat monitoring. It is important to understand under what conditions diurnal variations can be observed in VWC, to quantify their effect on microwave backscatter and the errors introduced in different applications if they are unaccounted for. Finally, observable diurnal differences in microwave backscatter due to variation in VWC could

Manuscript received February 4, 2014; revised June 11, 2014, July 22, 2014, and October 26, 2014; accepted November 21, 2014. The MicroWEX-11 experiment was supported by the National Aeronautics and Space Administration under Grant NASA-THP-NNX09AK29. The work of S. C. Steele-Dunne was supported by The Netherlands Organization for Scientific Research (NWO) Veni Grant Program (ALW 863.09.015).

T. van Emmerik, S. C. Steele-Dunne, and N. van de Giesen are with the Water Resources Section, Faculty of Civil Engineering and Geosciences, Delft University of Technology, 2628 CN Delft, The Netherlands.

J. Judge is with the Department of Agricultural and Biological Engineering, University of Florida, Gainesville, FL 32611 USA.

Color versions of one or more of the figures in this paper are available online at http://ieeexplore.ieee.org.

Digital Object Identifier 10.1109/TGRS.2014.2386142

be an interesting new source of information for hydrological, agricultural, and terrestrial ecosystem monitoring applications. Specifically, early detection of variation in VWC associated with the onset of water stress in agricultural crops could be useful for crop and water management and food security applications.

Several studies have found diurnal variation in backscatter due to VWC. Differences have been observed between morning and evening overpasses of backscatter observations from satellites [22], [23], aircraft, and ground-based platforms [24]–[26]. Frolking *et al.* [27] showed that the morning overpass of the SeaWinds scatterometer (13.4 GHz) on QuickSCAT was 0.5–1.0 dB higher than the evening overpass over the Amazon and used the diurnal differences as an indicator of water stress to study the 2005 drought in this region. Jaruwatanadilok and Stiles [28] found similar diurnal differences in SeaWinds data over other rain forests (Amazon, Congo, and Indonesia). Friesen [29] and Friesen *et al.* [30], [31] identified a statistically significant diurnal difference between the morning and evening passes of the ERS-1/2 wind scatterometer in vegetated areas. Friesen [29] used hydrological modeling to demonstrate that the timing and location of the largest difference between morning and evening measurements in West Africa coincided with the onset of water stress. Steele-Dunne *et al.* [32] performed a synthetic sensitivity study on a forest canopy using the Michigan Microwave Canopy Scattering (MIMICS) model [33], to investigate whether variations in leaf water content, and hence dielectric properties, could explain these differences in backscatter. Steele-Dunne *et al.* [32] confirmed that total backscatter from a forest canopy was sensitive to water content in both leaf and trunk, particularly around the onset of water stress when the soil is dry. This study also highlighted the lack of *in situ* data on diurnal variations in leaf water content for rigorous analyses.

In this paper, we characterize the diurnal variations in the VWC of an agricultural canopy and how these vary in response to water stress and quantify their impact on modeled backscatter for different frequencies, polarizations, and angles of incidence. Water stress was induced on a maize canopy in North Central Florida, between September 1 and October 20, 2012. A water-cloud model [34] was used with parameter sets obtained from three published experiments to investigate the influence of VWC variations on modeled backscatter for ranges of measured soil moisture and VWC, frequencies, polarizations, and incidence angles. Using measured diurnal VWC and soil moisture data, radar backscatter time series were simulated to investigate the effect of water stress and highlight the possible diurnal variation in backscatter due to changes in VWC.

II. Methods and Materials

A. Study Area

The fieldwork of this study was conducted at the University of Florida Plant Science Research and Education Unit, located in North Central Florida near Citra, FL, USA (N 29.41°, W 82.18°). Measurements were made as part of the Eleventh Microwave Water and Energy Balance Experiment (MicroWEX-11) from April 25 to December 9, 2012. For this research, sweet corn (*Zea mays L.*, 78-day growing period) was planted on a site of 183 m $\times$ 183 m, with 89% by volume fine sand, 1-m row spacing, and plant density of 5 plants/m. This study used observations during the late vegetative (maize is growing and developing [35]) and reproductive (maize is fully grown) periods, from September 1 to October 20, 2012. Typically, the crop is heavily irrigated due to sandy soils; however, there was no irrigation at the vegetation sampling location from September 29 to October 20, 2012. The growth of plants was restricted only by competition among plants.

B. Water Stress

1) Water Balance: Meteorological data, such as precipitation, soil and air temperature, relative humidity, wind speed, and solar radiation at the field site, were obtained from the Florida Automated Weather Network (FAWN), which is managed and maintained by the University of Florida (FAWN website: http://fawn.ifas.ufl.edu). All data were obtained from September 1 to October 20, 2012, with 15-min intervals.

To quantify water stress, a water balance was estimated using the following equation:

$$E_{\mathrm{def}} = E_{\mathrm{pot}} - (P + I) - \frac{\Delta S}{\Delta t} \tag{1}$$

where the evaporation deficit E_{def} $[\mathrm{mm} \cdot \mathrm{d}^{-1}]$ is determined as the difference between maximum potential evaporation E_{pot} $[\mathrm{mm} \cdot \mathrm{d}^{-1}]$ and the water available for evaporation, i.e., precipitation P $[\mathrm{mm} \cdot \mathrm{d}^{-1}]$, applied irrigation I $[\mathrm{mm} \cdot \mathrm{d}^{-1}]$, and soil moisture change $\Delta S/\Delta t$ $[\mathrm{mm} \cdot \mathrm{d}^{-1}]$.

The maximum potential evaporation was calculated using

$$E_{\mathrm{pot}} = E_{\mathrm{ref}} \cdot K_c \tag{2}$$

where E_{ref} $[\mathrm{mm} \cdot \mathrm{d}^{-1}]$ is the Penman–Monteith reference evaporation, and K_c $[-]$ is the Food and Agriculture Organization of the United Nations (FAO) crop factor for maize, which takes the growth stage into account [36]. From September 1 to 10, K_c was 0.3. Between September 10 and October 1, K_c increased linearly from 0.3 to 1.2, and between October 1 and 20, K_c was 1.2. Daily E_{ref} is provided by FAWN. The soil moisture profile was measured every 15 min, at six depths of 0.02, 0.04, 0.16, 0.32, 0.64, and 1.2 m, at the site, using Campbell Scientific CS616 time-domain water content reflectometers (Campbell Scientific, Inc., Logan, UT, USA). Soil moisture was measured several meters away from the vegetation sampling area. At the location of the soil moisture probes, irrigation continued until October 20, 2012. At the vegetation sampling location, the last irrigation event was on September 29, 2012. Therefore, the evaporation deficit calculated using the soil moisture measurements underestimates the evaporation deficit at the vegetation sampling location, providing a conservative estimate of the degree of water stress.

2) Soil Water Tension: Soil water tension was measured at the vegetation sampling location from September 11 to October 19, 2012, using two UMS T4/e pressure transducer tensiometers (UMS GmbH, Munich, Germany). One was installed

at 50 cm, with an angle of 35° with respect to the vertical, and one was installed at 30-cm depths, with an angle of 40°.

C. VWC

The VWC was measured at 6 A.M. and 6 P.M. in 19 days, from September 24 to October 19, 2012. Concurrently, two maize plants were cut, weighed with leaves and stalks separated, dried in a 70 °C oven for 48 and 120 h, respectively, and weighed again. VWC values were determined from the fresh and dry masses (m_f and m_d), using the following equation:

$$\text{VWC} = \eta\left[(m_{f,l} - m_{d,l}) + (m_{f,s} - m_{d,s})\right] \tag{3}$$

where η is the number of plants per square meter, and the superscripts l and s indicate leaves and stalks.

D. Water-Cloud Model

Radar is influenced by vegetation by three main mechanisms [37]: direct backscatter from plants, two-way attenuation of soil backscatter, and the multiple scattering between soil and vegetation. For this study, the water-cloud model [34] was used to estimate radar backscatter, which assumes that a canopy can be represented by a cloud of randomly distributed water droplets, based on the assumption that the vegetation dielectric constant is dominated by the dielectric constant of water.

Here, we use three published data sets [5], [37], [38], each of which requires a slightly different form of the original water-cloud model of Attema and Ulaby [34]. To allow a comparison between model output of all different radar frequencies, incidence angles, and polarizations, vegetation and soil backscatter were calculated separately. Vegetation backscatter was determined based on the equations provided by the individual models. For soil backscatter contribution, the bare soil scattering model of Dubois *et al.* [2] was used.

All modeled backscatter will be presented in decibels [dB]. The water-cloud parameters used in the three modeling approaches can be found in Table I. To evaluate the diurnal differences in modeled radar backscatter for different frequencies, polarizations, and incidence angles, a T-test was performed to determine the statistical significance. This was also done for the morning and evening values for VWC and soil moisture.

1) L-Band (HH, 35°) and C-Band (VV, 23°): Dabrowska-Zielinska *et al.* [38] used a simplified water-cloud model, based on [39] and [40], to simulate C-band (VV, 23°) and L-band (HH, 35°) radar backscatter. Total backscatter σ^0_{tot} is described as

$$\sigma^0_{\text{tot}} = \sigma^0_{\text{veg}} + \gamma^2\sigma^0_{\text{soil}} \tag{4}$$

with vegetation contribution σ^0_{veg}, soil contribution σ^0_{soil}, and two-way attenuation γ^2. σ^0_{veg} and γ^2 are formulated as

$$\sigma^0_{\text{veg}} = AV_1^E\cos\theta(1-\gamma^2) \tag{5}$$

$$\gamma^2 = \exp\left(\frac{-2BV_2}{\cos\theta}\right) \tag{6}$$

with model parameters A, B, and E; incidence angle θ; and VWC V_1 and V_2 [4], [6], [39]. Model parameters A, B, and E are parameters depending on the used radar frequency, incidence angle, polarization, and crop.

2) C-Band (HH and VV, 15°, 35°, and 55°): The water-cloud model of Joseph *et al.* [5] is similar to those of Bindlish and Barros [6] and Ulaby *et al.* [37]. Joseph *et al.* [5] calibrated their model for C-band backscatter with HH and VV polarization and three incidence angles, i.e., 15°, 35°, and 55°. σ^0_{tot} is given by (4). The vegetation term is formulated as

$$\sigma^0_{\text{veg}} = (1-\gamma^2)AV_1\cos\theta \tag{7}$$

with VWC V_1, model parameters A, and E and incidence angle θ. The two-way attenuation is determined using (6).

3) X-, K_u-, and K_a-Band (VV, 50°): Ulaby *et al.* [37] account for the leaves and stalks separately, such that total backscatter σ^0_{tot} is given by

$$\sigma^0_{\text{tot}} = \sigma^0_{\text{leaf}} + \sigma^0_{\text{stalk}} + \sigma^0_{\text{soil}} \tag{8}$$

with leaf and stalk backscatter σ^0_{leaf} and σ^0_{stalk}, respectively, and soil contribution σ^0_{soil}. σ^0_{leaf} and σ^0_{stalk} are given by

$$\sigma^0_{\text{leaf}} = A_{\text{leaf}}\left[1-\exp\left(\frac{-B_{\text{leaf}}V_1}{h_1}\right)\right]\left[1-\gamma^2_{\text{leaf}}\right]\cos\theta \tag{9}$$

$$\sigma^0_{\text{stalk}} = A_{\text{stalk}}\cdot V_2\cdot\frac{h_2}{h}\cdot\gamma^2_{\text{leaf}} \tag{10}$$

with leaf vegetation parameters A_{leaf} and B_{leaf}, leaf VWC V_1, height of the leaf layer h_1 (see Fig. 1), leaf attenuation factor γ^2_{leaf}, angle of incidence θ, stalk vegetation parameters A_{st}, stalk VWC V_2, height of the stalk layer h_2, and total plant height h (see Fig. 1). The leaf and stalk attenuation factors γ^2_{leaf} and γ^2_{stalk} determine how much of the original signal made is attenuated by the leaf and stalk layer and are given by

$$\gamma^2_{\text{leaf}} = \exp(-2\cdot\alpha_{\text{leaf}}\cdot\sec\theta V_1) \tag{11}$$

$$\gamma^2_{\text{stalk}} = \exp\left(-\alpha_{\text{stalk}}\cdot V_2\cdot\frac{h_2}{h}\right) \tag{12}$$

with model parameters α_{leaf} and α_{stalk}.

From October 7 to 21, the ratio of leaf water content over bulk water content was 0.20, with a standard deviation of 0.05. For the sensitivity study, this value is used to separate bulk VWC into leaf and stalk water content.

4) Soil Backscatter: This empirical backscattering approach is based on field data sets, and describes HH- or VV-polarized radar backscatter as a function of the angle of incidence θ, frequency f, surface roughness h, wavenumber k, the dielectric constant of soil ϵ, and wavelength λ, using the following equations:

$$\sigma^0_{\text{hh}} = 10^{-2.75}\cdot\frac{\cos^{1.5}\theta}{\sin^5\theta}\cdot 10^{0.028\epsilon\cdot\tan\theta}(kh\sin\theta)^{1.4}\cdot\lambda^{0.7} \tag{13}$$

$$\sigma^0_{\text{vv}} = 10^{-2.35}\cdot\frac{\cos^3\theta}{\sin^3\theta}\cdot 10^{0.046\epsilon\cdot\tan\theta}(kh\sin\theta)^{1.1}\cdot\lambda^{0.7}. \tag{14}$$

TABLE I
USED PARAMETERS FOR WATER-CLOUD MODELS

Model	Radar parameters				Vegetation parameters					
	Band	Freq. [GHz]	Angle [°]	Pol.	A	B	α	E	A_{st}	α_{st}
Ulaby *et al.* (1984)	X	8.6	50	VV	0.22	2.6	0,411		0.025	0
	K_u	17	50	VV	0.30	2.7	0,418		0.022	0
	K_a	35	50	VV	0.36	2.0	0,360		0.034	0
Dabrowska-Zielinska *et al.* (2007)	L	1.275	35	HH	0.01	0.04		0.0		
	C	5.3	23	VV	0.08	0.15		2.9		
Joseph *et al.* (2010)	C	4.8	15	HH	0.03	0.09				
	C	4.8	15	VV	0.01	0.13				
	C	4.8	35	HH	15.96	$1.18 \cdot 10^{-4}$				
	C	4.8	35	VV	3.05	$1.38 \cdot 10^{-4}$				
	C	4.8	55	HH	5.57	$4.16 \cdot 10^{-4}$				
	C	4.8	55	VV	2.96	$1.96 \cdot 10^{-4}$				

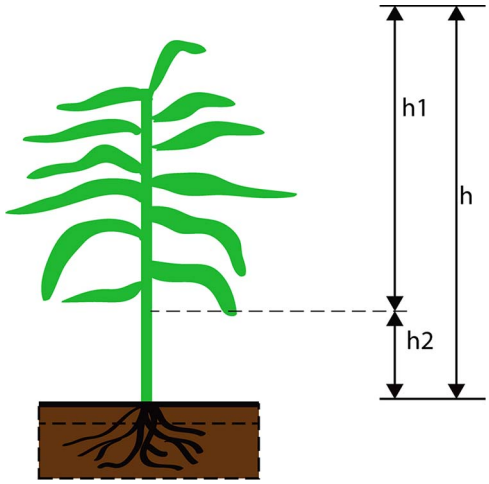

Fig. 1. Vegetation heights h, h_1, and h_2 as used in the water-cloud model.

A value for root-mean-square height ($h = 1$ cm) was assumed for the entire period. This value is based on reported values in the literature for similar conditions [4], [5], [41], [42]. Soil dielectric constant was computed using the dielectric mixing model, as presented by Dobson [43]. Dielectric constants varied between 3.4 and 5.7, for the surface soil moisture values measured between 0.04 and 0.15.

III. RESULTS AND DISCUSSION

A. Water Stress

Fig. 2(a) shows rainfall and irrigation. In the last week of September, irrigation was necessary to ensure that the maize had enough moisture during the end of the growing phase. After October 7, irrigation was withheld at the vegetation sampling area to induce water stress. Fig. 2(b) shows the volumetric soil moisture profile in the soil over time. It is clear that this sandy soil remained very dry for the duration of the experiment. After September 30, near-surface soil moisture varied between 0.04 and 0.15 $m^3 \cdot m^{-3}$ at the near surface (0.02-m depth) and between 0.08 and 0.09 $m^3 \cdot m^{-3}$ at 1.2 m. Increases in near-surface soil moisture were observed on October 9, 12, 15, and 19. Because the soil moisture sensors were placed outside the vegetation sampling area, the available soil moisture is overestimated. Fig. 2(c) shows the surface soil moisture values at 6 A.M. and 6 P.M. Peaks are observed after rainfall or irrigation events. Fig. 2(d) shows the calculated daily evaporation decreasing with time. The evaporation deficit, an indicator of water stress in this study, is shown in Fig. 2(e). The deficit increases gradually until October 7 because irrigation is provided to supplement the precipitation. After October 7, the cumulative evaporation deficit increases rapidly in the absence of irrigation. For comparison, Fig. 2(e) shows the soil water tension measured at 30 and 50 cm. The values measured are consistent with the published values for dry sandy soils [44] [45]. The dynamics of soil water tension reflect those of the moisture in Fig. 2(b), with drier soil and higher soil water tension closer to the surface. The soil water tension at depth exhibits a slower and damped response to the absence of precipitation or irrigation. After October 7, soil tension at 30 and 50 cm increases in agreement with the rising cumulative evaporation deficit. The rapid increase in cumulative evaporation deficit is particularly apparent in the soil water tension at 30 cm.

Table II shows the statistical significance of diurnal variation in VWC and soil moisture. Low values (< 0.9) mean an absence of statistically significant diurnal variation. No statistically significant diurnal difference in soil moisture was observed. Because soil moisture was measured in the irrigated field, diurnal differences might have occurred at the vegetation sampling size. However, since irrigation was absent, it is assumed that, if present, these variations are very low. Observed diurnal differences in VWC were clearly significant.

B. VWC

The VWC is shown in Fig. 3. Fig. 3(a) shows the bulk VWC, and Fig. 3(b) shows the VWC for stalks and leaves separately. As the maize reaches the final vegetative stages (V10 and V11), most of the water in the plant is stored in the stalks. Consequently, the temporal variations in bulk and stalk VWC are very similar. Up to October 7, the maize is still developing and growing, and therefore, the stalk and bulk VWC increases. After the maize is fully developed, the increasing water stress causes a decrease in stalk and bulk VWC. The leaf VWC is quite stable until September 30 but then shows a decreasing trend from the onset of water stress onward.

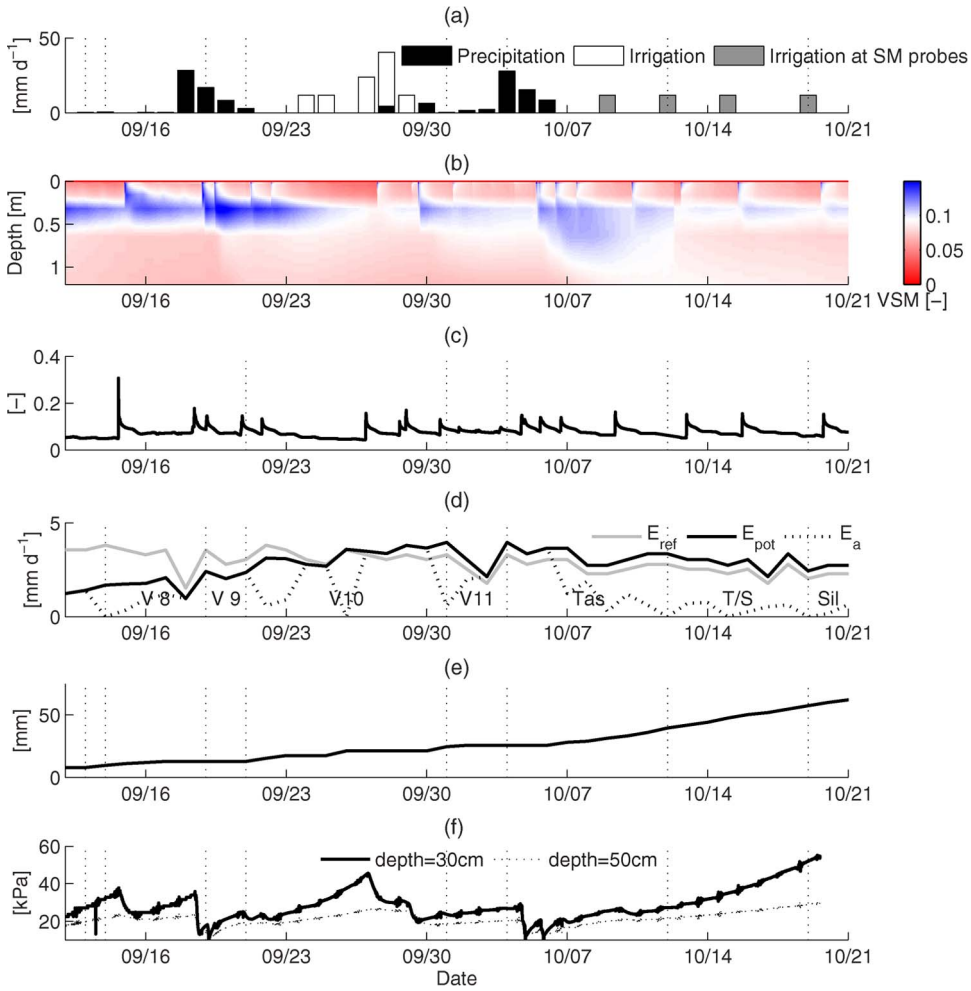

Fig. 2. (a) Precipitation and irrigation at the measurement site. (b) Soil moisture profile over time. (c) Surface soil moisture over time. (d) Calculated daily evaporation at the measurement site. (e) Water stress quantified by cumulative evaporation deficit. (f) Water stress quantified by soil water tension at 30- and 50-cm depths.

TABLE II
T-TEST RESULTS TO DETERMINE STATISTICAL SIGNIFICANCE OF DIURNAL DIFFERENCES: (−) MEANS A DECREASE BETWEEN 6 A.M. AND 6 P.M., AND (+) MEANS AN INCREASE BETWEEN 6 A.M. AND 6 P.M. DIURNAL DIFFERENCES ARE STATISTICALLY SIGNIFICANT FOR $1 - P \geq 0.9$

Model	Radar parameters				T-test	
	Band	Freq. [GHz]	Angle [°]	Pol.	1 - P	+/-
Ulaby *et al.* (1984)	X	8.6	50	VV	1.00	-
	K_u	17	50	VV	1.00	-
	K_a	35	50	VV	1.00	-
Dabrowska-Zielinska *et al.* (2007)	L	1.275	35	HH	0.98	-
	C	5.3	23	VV	0.92	+
Joseph *et al.* (2010)	C	4.8	15	HH	0.97	+
	C	4.8	15	VV	0.96	+
	C	4.8	35	HH	0.99	-
	C	4.8	35	VV	0.83	-
	C	4.8	55	HH	0.98	-
	C	4.8	55	VV	0.87	-
Surface soil moisture					0.06	-
Total soil moisture					0.08	+
Bulk VWC					0.98	-
Leaf VWC					1.00	-
Stalk VWC					0.89	-

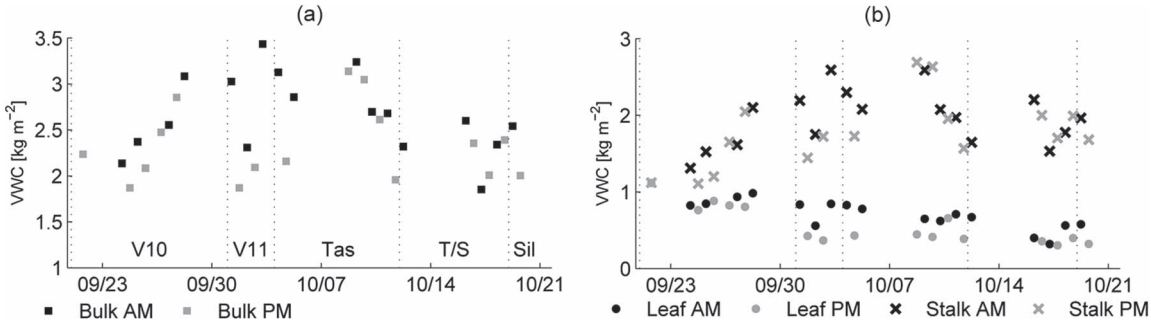

Fig. 3. Results of vegetation sampling. (a) Bulk VWC at 6 A.M. and 6 P.M. (b) Leaf and stalk VWC at 6 A.M. and 6 P.M.

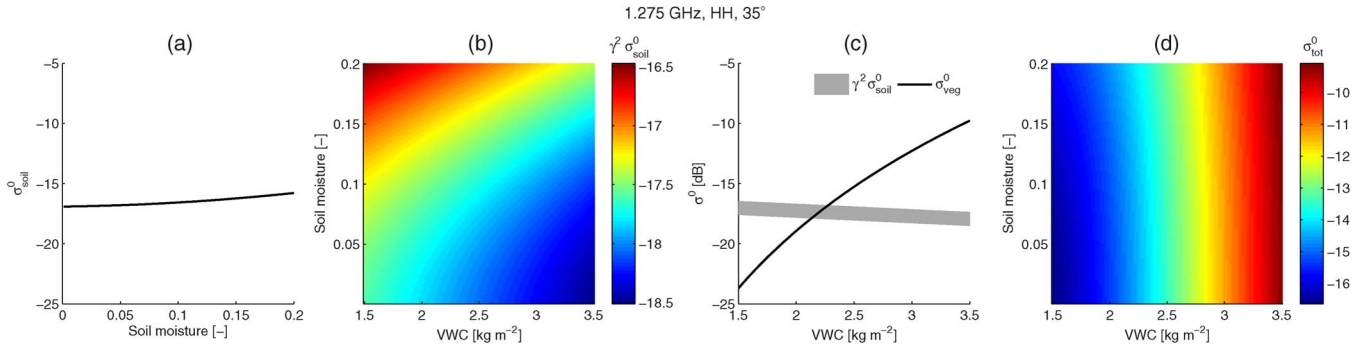

Fig. 4. Sensitivity of L-band (1.275 GHz, HH, 35°) radar backscatter modeled using Dabrowska-Zielinska *et al.* [38] to soil moisture and VWC. (a) Soil backscatter as function of soil moisture. (b) Attenuated soil backscatter as function of VWC and soil moisture. (c) Vegetation backscatter as function of VWC, including the range of the attenuated soil backscatter contribution. (d) Total backscatter as function of VWC and soil moisture.

In 13 days, leaf and stalk VWC was measured at both 6 A.M. and 6 P.M. The VWC of leaves and stalks was higher at 6 A.M. than at 6 P.M. in eleven and nine days, respectively. On October 17 and 18, the evening bulk VWC was higher than the morning VWC. This is unexpected since, on most days, VWC decreased during 6 A.M. and 6 P.M. It is likely that the observed increase is due to spatial variation. In particular, on October 17, a relatively low VWC was observed in the morning.

Diurnal differences in total VWC were statistically significant (see Table II). This was expected since transpiration of maize occurs mainly during the day, with the peak transpiration rate around noon, causing the VWC of maize to decrease between morning and evening. The morning leaf measurements decrease as stress continues, suggesting that the plant cannot replenish all water lost during the day. The trend is less significant in the evening leaf measurements.

C. Backscatter Sensitivity Study

1) Dabrowska-Zielinska et al. (2007): Fig. 4 shows the horizontally copolarized backscatter at 1.275 GHz and an incidence angle of 35°, simulated using (4)–(6) and the parameters from the water-cloud model of Dabrowska-Zielinska *et al.* (see Table I). During the observation period, surface soil moisture was low (between 0.04 and 0.15 $m^3 \cdot m^{-3}$); hence, the range of backscatter from bare soil is about 1.5 dB [see Fig. 4(a)]. VWC varies between 1.7 and 3.5 $kg \cdot m^{-2}$, which leads to a range of around 2 dB in attenuated soil backscatter [see Fig. 4(b)]. Fig. 4(c) illustrates that backscatter from the vegetation itself varies between -24 and -10 dB, which is considerably larger than the range of values simulated for the attenuated soil backscatter. Furthermore, at VWC values greater than 2.3 $kg \cdot m^{-2}$, σ°_{veg} is greater than $\gamma^2\sigma^\circ_{soil}$. Consequently, total backscatter dynamics are primarily a function of VWC, as shown in Fig. 4(d).

VWC affects the transparency of the canopy layer. At an incidence angle of 35°, changes in soil moisture have a small effect on total backscatter because the path through the canopy layer is large [46, Sec. 11-5]. Increasing VWC will decrease the penetration capacity. At L-band, low VWC makes vegetation transparent, and the soil moisture signal governs total backscatter. However, the effect of changes in soil moisture on backscatter is limited. High VWC results in a low penetration capacity; hence, the backscatter signal mainly consists of vegetation contribution. In case soil moisture variation is low, backscatter mainly reflects the dynamics in VWC. Dabrowska-Zielinska *et al.* [38] investigated the effect of plant and soil variables on L-band radar. It was found that, for L-band (35°), the dominant signal to total backscatter comes from vegetation, in case of VWC greater than 3 $kg \cdot m^{-2}$ and soil moisture varying between 0 and 0.6. We measured surface soil moisture between 0.04 and 0.15 and VWC between 1.7 and 3.5 $kg \cdot m^{-2}$. Compared to [38], we show that, in case of low soil moisture variability, total backscatter is also mainly sensitive to variations in VWC within this lower range. This is interesting because this means that the effect of VWC on L-band radar backscatter might be larger than previously found. We show that, particularly at times of low soil moisture variability, total backscatter is mainly influenced by dynamics in VWC.

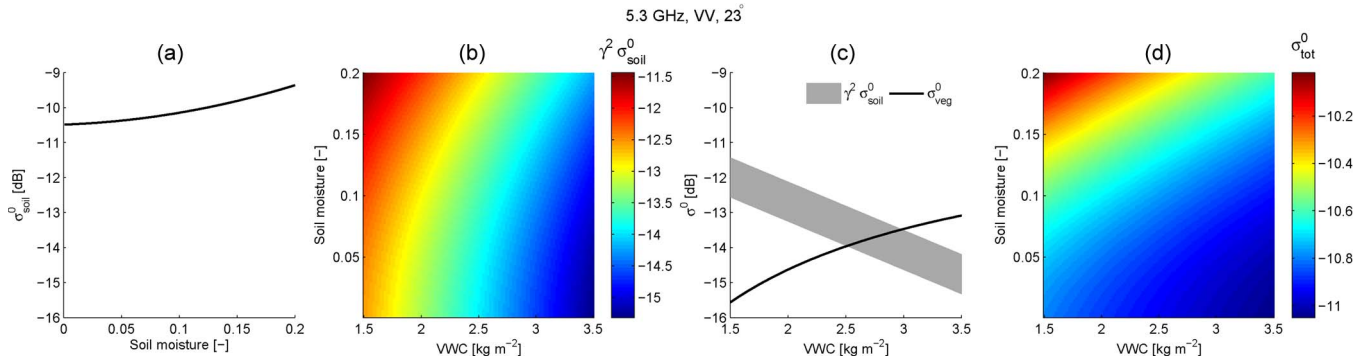

Fig. 5. Sensitivity of C-band (5.3 GHz, VV, 23°) radar backscatter, using Dabrowska-Zielinska *et al.* [38], to soil moisture and VWC. (a) Soil backscatter as function of soil moisture. (b) Attenuated soil backscatter as function of VWC and soil moisture. (c) Vegetation backscatter as function of VWC, including the range of the attenuated soil backscatter contribution. (d) Total backscatter as function of VWC and soil moisture.

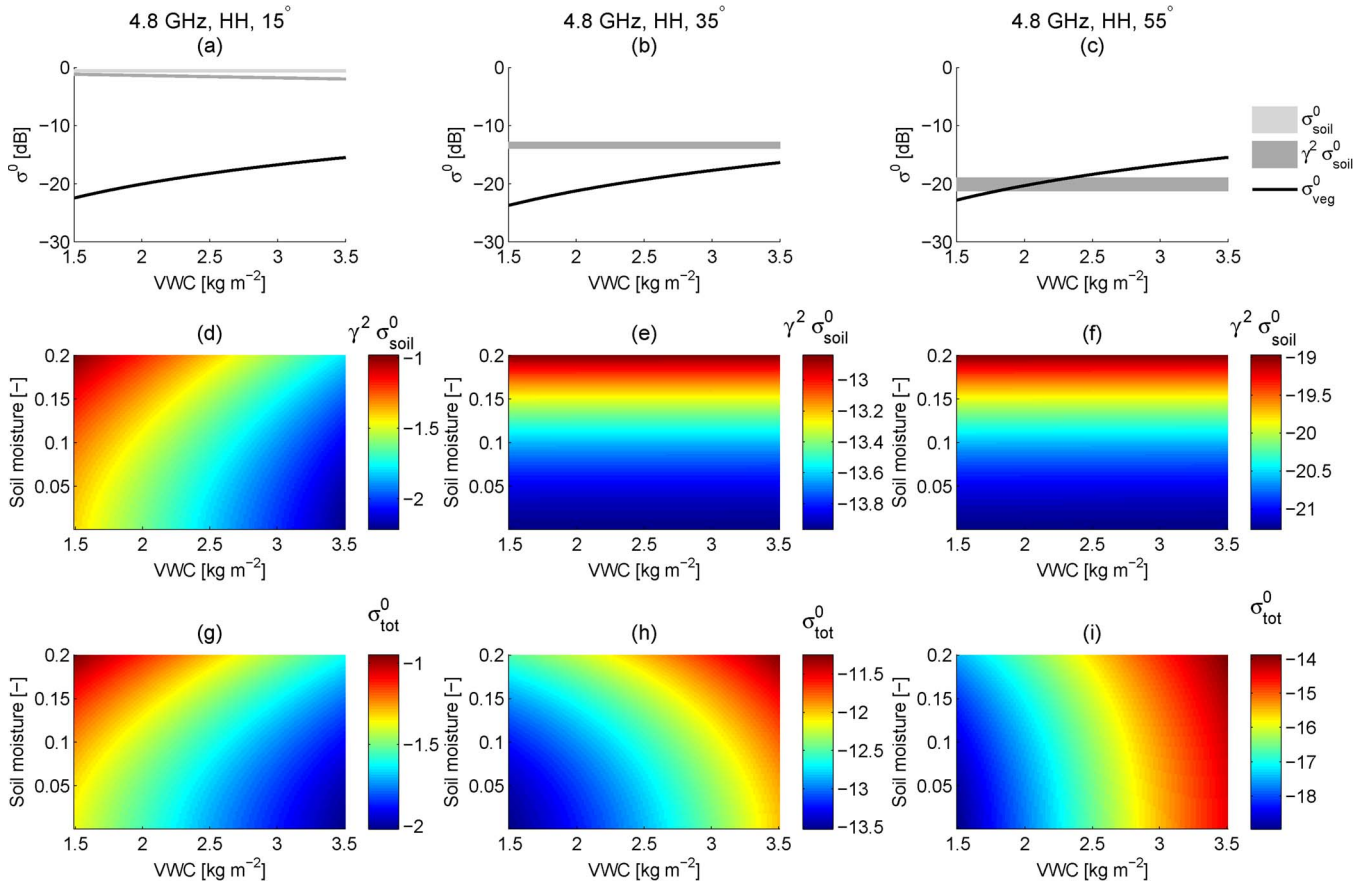

Fig. 6. Sensitivity of C-band (4.8 GHz) horizontally polarized radar backscatter at different incidence angles using Joseph *et al.* [4]. (a)–(c) Vegetation and attenuated soil contributions as a function of VWC for 15°, 35°, and 55°, respectively. (d)–(f) Attenuated soil backscatter as a function of VWC and soil moisture for 15°, 35°, and 55°, respectively. (g)–(i) Total backscatter as a function of VWC and soil moisture for 15°, 35°, and 55°, respectively.

Fig. 5 shows the vertically copolarized backscatter at 5.3 GHz and an incidence angle of 23°, for the same model and appropriate parameters in Table I. In this case, the range of attenuated soil backscatter for a given value of VWC is 3.5 dB, which is larger than the range of simulated $\sigma^{\circ}_{\mathrm{veg}}$ values (2.5-dB variation). The magnitudes of the two backscatter terms are comparable, with the vegetation term dominating when VWC exceeds 3.0 $\mathrm{kg} \cdot \mathrm{m}^{-2}$. As a result, total backscatter is sensitive to both VWC and soil moisture [see Fig. 5(d)]. Because the incidence angle is relatively low, the path through the vegetation is short. Closer to nadir, agricultural canopies are more transparent, and microwaves can more easily penetrate through the vegetation layer. Therefore, backscatter is relatively sensitive to changes in soil moisture. However, higher VWC leads to a lower penetration capacity, and the contribution from vegetation is larger than the soil contribution. Dabrowska–Zielinska *et al.* [38] found that, for VWC equal to 5 $\mathrm{kg} \cdot \mathrm{m}^{-2}$, soil contributes 50% to total backscatter, mainly due to larger soil moisture variations (0–0.6). We show that this is also the case for lower values of VWC.

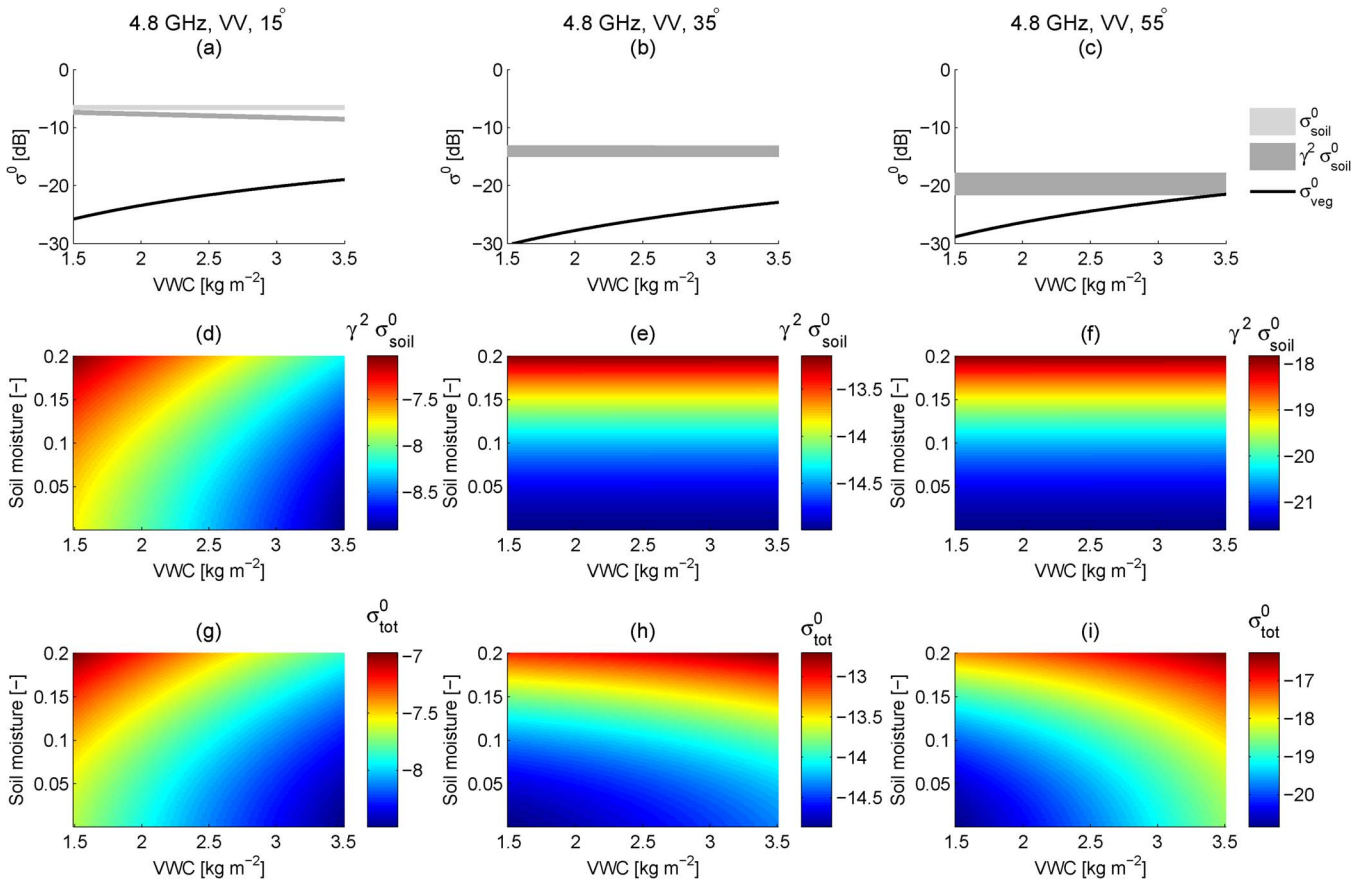

Fig. 7. Sensitivity of C-band (4.8 GHz) vertically polarized radar backscatter at different incidence angles using Joseph *et al.* [4]. (a)–(c) Vegetation and attenuated soil contributions as a function of VWC for 15°, 35°, and 55°, respectively. (d)–(f) Attenuated soil backscatter as a function of VWC and soil moisture for 15°, 35°, and 55°, respectively. (g)–(i) Total backscatter as a function of VWC and soil moisture for 15°, 35°, and 55°, respectively.

Between 2.5 and 3.0 kg · m^{-2}, soil contributes 50% to total backscatter. For VWC higher than 3.0 kg · m^{-2}, the vegetation is the main contributor to total backscatter. In the range of VWC and soil moisture observed, Fig. 5 shows that C-band (VV, 23°) total backscatter is sensitive to both VWC and soil moisture.

The modeled sensitivity of backscatter to diurnal variation in VWC was done for agricultural canopies. Interestingly, for various vegetation types, a strong sensitivity of backscatter to diurnal dynamics in VWC has been found in case of low soil moisture variation. Over savannas in West Africa, Friesen *et al.* [31] found a statistically significant diurnal difference in ERS backscatter and hypothesized that this was caused by diurnal variation in VWC. For tree forests, Steele-Dunne *et al.* [32] showed that, at L- and C-band, changes in leaf moisture lead to a significant change in total backscatter over a forest canopy. Although agricultural canopies are less densely vegetated than forests, the results in this paper show that total backscatter at L- and C-band is sensitive to both VWC and soil moisture. During periods of water stress, soil moisture is likely to be low and change slightly during the day; hence, total backscatter will be mainly influenced by VWC dynamics of savannas, forests, and agricultural canopies.

2) Influence of Incidence Angle at C-Band: Here, results are presented for C-band (4.8 GHz) vertically and horizontally copolarized backscatter for three different incidence angles, simulated using (4)–(7) and the parameters from [5] provided in Table I.

Fig. 6 shows the simulated horizontally copolarized backscatter at 15°, 35°, and 55°, for the observed range of surface soil moisture and VWC. In Fig. 6(a)–(c), the direct vegetation contribution is similar (−15 to −22 dB) for all three incidence angles. The magnitude of the attenuated soil backscatter decreases from −6.5 dB at 15° to −21.5 dB at 55°. As shown in Fig. 6(d)–(f), the influence of VWC on the attenuated soil backscatter is different at low and high incidence angles. At 15° [see Fig. 6(d)], the attenuated soil backscatter decreases considerably with increasing VWC. At 35° and 55°, the path through the vegetation is longer, and the water-cloud model vegetation parameter B (representing the extinction coefficient for a canopy [46, Sec. 11-5]) is very small (see Table I); hence, γ^2 is close to unity and independent of VWC.

It was expected that attenuation γ^2 would have been higher for increasing incidence angles, leading to more attenuation of σ^0_{soil}. The reason for low γ^2 can be found in the calibration of the water-cloud model, where parameter A was significantly higher at 35° and 55°, leading to higher σ^0_{veg} and lower γ^2. When one looks at the total backscatter modeled by Joseph *et al.* [5], the complete effect of vegetation is captured (direct backscatter and attenuation). However, these parameter

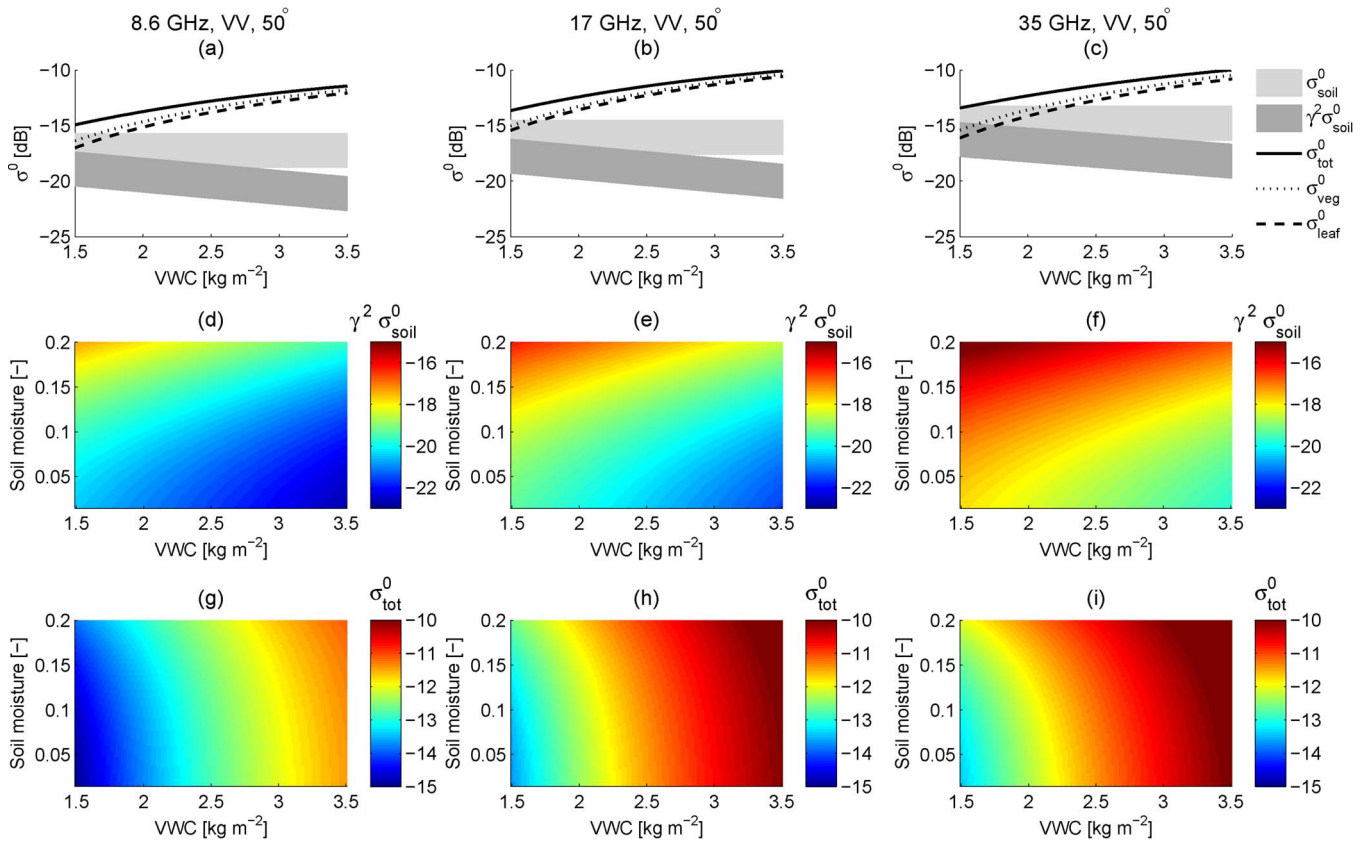

Fig. 8. Sensitivity of radar backscatter at 8.6 GHz (a, d, g), 17 GHz (b, e, h), and 35 GHz (c, f, i) to soil moisture and VWC using Ulaby *et al.* [37]. (a)–(c) Total and leaf vegetation backscatter and range of soil and attenuated soil backscatter of as function of VWC. (d)–(f) Attenuated soil backscatter as function of soil moisture and VWC. (e)–(i) Total backscatter as function of soil moisture and VWC.

sets do not capture the dynamics of the individual contributions from soil and vegetation. At 15°, total backscatter is dominated by the attenuated soil backscatter [see Fig. 6(a)]; hence, total backscatter [see Fig. 6(g)] depends on both soil moisture and VWC. At this incidence angle, a decrease in VWC would lead to an increase in backscatter. Interestingly, at 55° and HH polarization, the direct backscatter from the canopy (highly sensitive to VWC) is similar in magnitude to the attenuated soil backscatter (insensitive to VWC). As the incidence angle increases, total backscatter becomes increasingly sensitive to VWC. At 35° and 55°, a decrease in VWC leads to a decrease in total backscatter.

Similar results were obtained for vertically copolarized C-band backscatter (see Fig. 7). In this case, even at the larger incidence angles, the attenuated soil backscatter dominates; hence, the total backscatter at 35° and 55° is less sensitive to VWC than the horizontally copolarized case.

Joseph *et al.* [5] also found that, for increasing incidence angles, changes in backscatter showed more resemblance to changes in VWC and less to variation in soil moisture. Horizontally copolarized backscatter was more sensitive to changes in VWC at 35° and 55° than vertically copolarized backscatter. Ulaby *et al.* [46, Sec. 11-5] found that the sensitivity to soil moisture over an agricultural canopy decreases with an increasing incidence angle. Total backscatter also decreased with increasing incidence angles because, at higher angles, the path through vegetation increases and the penetration capacity decreases. A larger portion of the incoming microwaves will scatter and not make it to the soil.

Joseph *et al.* [5] found that, at 15°, attenuated soil is the more dominant contributor to total backscatter and that, at 35° and 55°, scattering from vegetation becomes more dominant. It was mentioned that, for VWC equal to 5.1 kg · m^{-2}, backscatter was sensitive to changes in soil moisture. Our results add that, for 15°–55° and low variation in soil moisture (0–0.2), changes in VWC (1.5–3.5 kg · m^{-2}) can also affect total backscatter. This is particularly evident in C-band horizontally copolarized backscatter (see Fig. 6) and becomes more significant with increasing incidence angle. Rather than looking at vegetation as something to correct for in soil moisture retrieval algorithms, this suggests that the sensitivity of radar to changes in VWC might also be a new source of information.

3) High Frequencies: Fig. 8 shows the sensitivity of high-frequency (8.6, 17, and 35 GHz; VV-polarized; 50°) radar backscatter to soil moisture and VWC. Fig. 8(a)–(c) shows that the direct vegetation backscatter is equal to the backscatter from the leaves at all frequencies. For increasing frequencies, the magnitude of the vegetation contribution increases from −17 to −12 dB at 8.6 GHz to −16 to −10 dB at 35 GHz. This corresponds to the original results presented by Ulaby *et al.* (1984) [37], where it was found that the variation in backscatter over a maize field is higher for increasing frequencies. The attenuated soil backscatter is smaller than the vegetation term [see Fig. 8(d)–(f)] for VWC below 1.5 kg · m^{-2} at 8.6 and

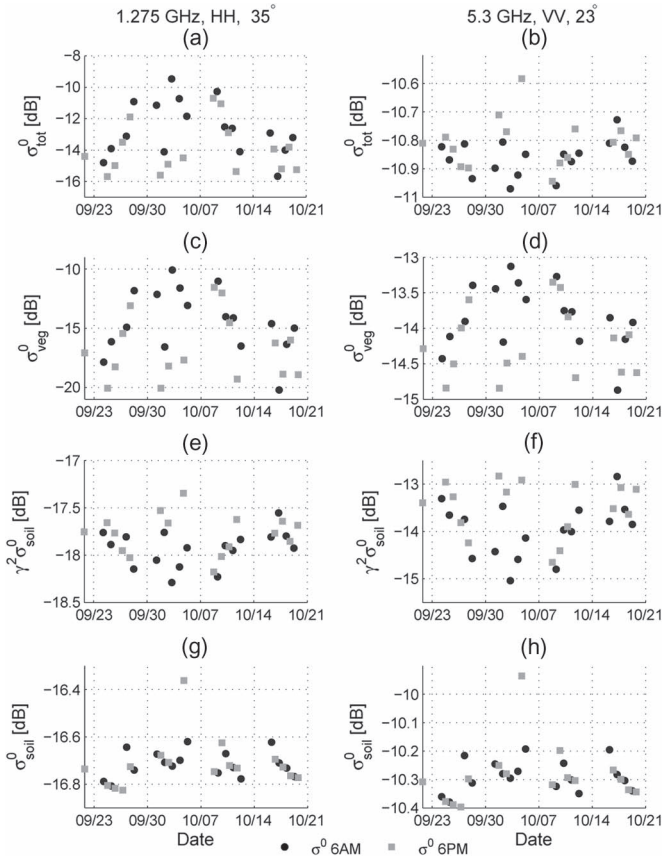

Fig. 9. Modeled radar backscatter time series at L-band (1.275 GHz, HH, 35°) and C-band (5.3 GHz, VV, 23°) using Dabrowska-Zielinska *et al.* [38]: (a) and (b) total backscatter, (c) and (d) vegetation contribution, (e) and (f) attenuated soil backscatter, and (g) and (h) soil contribution.

17 GHz and 1.7 kg · m^{-2} at 35 GHz. Consequently, the total backscatter is primarily sensitive to VWC, or more precisely to leaf VWC. At high frequencies, a larger fraction of the incoming microwaves will be scattered by the canopy surface. A lower amount of volume scattering thus means a lower sensitivity to total VWC, since from our results, it can be seen that leaf VWC mainly determines the amount of surface scattering. This is particularly interesting because the results in Fig. 3 illustrate that the dynamics of leaf VWC are different from those of bulk VWC.

D. Time Series of Modeled Radar Backscatter

1) Dabrowska-Zielinska et al. (2007): Fig. 9(a) shows the time series of L-band (35°, HH) total backscatter simulated using (4)–(7) and the parameters from Dabrowska-Zielinska *et al.* [38]. Fig. 9(c), (e), and (g) shows the contributions from vegetation, attenuated soil, and soil backscatter, respectively.

Fig. 9(g) shows the variation in $\sigma^0_{\rm soil}$ due to the limited variations observed in surface soil moisture. Recall that soil moisture was measured in the irrigated field. While no diurnal differences were observed there (see Table II), they may have occurred at the vegetation sampling site. However, in the absence of irrigation, it is reasonable to assume that variability in surface soil moisture at the vegetated sampling site would be even less than that observed at the irrigated field. For the observed variation in soil moisture, the range of simulated backscatter from the soil is about 0.4 dB. Fig. 9(e) shows the impact of the measured variations in VWC on the simulated attenuated soil backscatter. The difference in dynamics between Fig. 9(e) and (g) is due to the measured variations in VWC. In nine days, $\gamma^2\sigma^0_{\rm soil}$ was lower at 6 A.M. than at 6 P.M. due to diurnal variations in VWC, although the total range of values is less than 1 dB. Recall in Fig. 4(c) that the range of simulated vegetation backscatter at L-band (35°, HH) is 13 dB for the range of observed VWC and that, above VWC = 2.3 kg · m^{-2}, this term is the dominant contribution to total backscatter. Hence, the variations in $\sigma^0_{\rm veg}$ [Fig. 9(c)] are due to the observed changes in the bulk VWC. In late September, the VWC increases as the plants grow, which results in an increase in $\sigma^0_{\rm veg}$. The decline in VWC after October 7 results in a decrease in $\sigma^0_{\rm veg}$. Vegetation backscatter is significantly higher in the morning than in the evening due to the diurnal difference in VWC (see Table II), with differences of up to 7 dB between October 1 and 20, 2012. In Fig. 9(a) and (c), it is clear that diurnal variations observed in VWC dominate the simulated dynamics in total L-band (35°, HH) backscatter and explain the statistically significant difference simulated between 6 A.M. and 6 P.M. values.

It is generally accepted that the L-band penetrates further through canopies (e.g., [4] and [47]). Ulaby *et al.* [46] showed that, at increasing incidence angles, the penetration through canopy decreases, resulting in a lower sensitivity to soil moisture. Fig. 9 shows that, at a 35° incidence angle and HH copolarization, the effect of vegetation and its diurnal dynamics cannot be neglected in case of low soil moisture variability. Both attenuation and direct backscatter caused by diurnal variation in VWC can have a significant influence on total backscatter. In Table II, it can be seen that diurnal differences in L-band backscatter are statistically significant. This is interesting for soil moisture and vegetation monitoring using L-band radar. Before, the main focus was on soil moisture, attributing variation in backscatter to changes in soil moisture. However, Fig. 9(a) shows that, during times of low soil moisture availability, diurnal differences in L-band (35°, HH) backscatter can be attributed to changes in VWC. This does not only highlight potential errors in soil moisture retrieval algorithms, but it also points out the potential of radar for vegetation and water stress monitoring.

At C-band (23°, VV), the range of total backscatter values over the whole time series, as shown in Fig. 9(b), is just 0.4 dB. Recall in Fig. 5 that the total backscatter in this configuration was dominated by the attenuated soil moisture signal up to a VWC of 3 kg · m^{-2}. The limited variation in measured surface soil moisture results in a range in simulated $\sigma^0_{\rm soil}$ of less than 0.4 dB [see Fig. 9(h)]. The impact of VWC in attenuating this soil signal is shown in Fig. 9(f). Simulated attenuated soil backscatter is up to 2 dB lower in the morning due to the diurnal variations in measured VWC. The VWC has an opposite effect on $\sigma^0_{\rm veg}$, with higher 6 A.M. VWC values producing simulated $\sigma^0_{\rm veg}$ up to 1.5 dB higher in the morning. Recall in Fig. 5(d) that these two effects are comparable in magnitude. Hence, there is limited variation in simulated total C-band (23°, VV) backscatter. Although Table II shows that there is a statistically

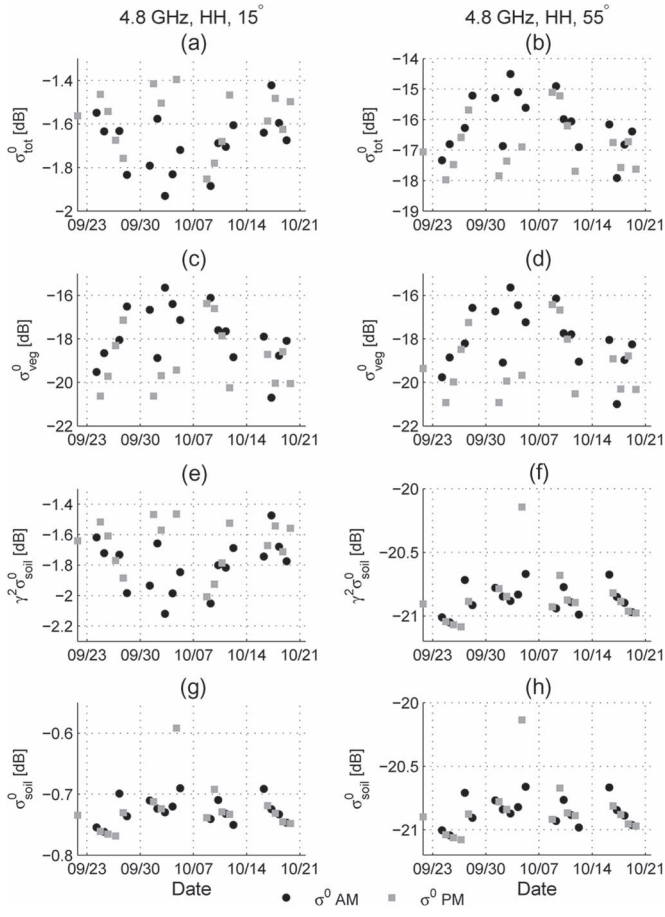

Fig. 10. Modeled radar backscatter time series at horizontally polarized C-band (4.8 GHz) using Joseph *et al.* [5]: (a) and (b) total backscatter, (c) and (d) vegetation contribution, (e) and (f) attenuated soil backscatter, and (g) and (h) soil contribution.

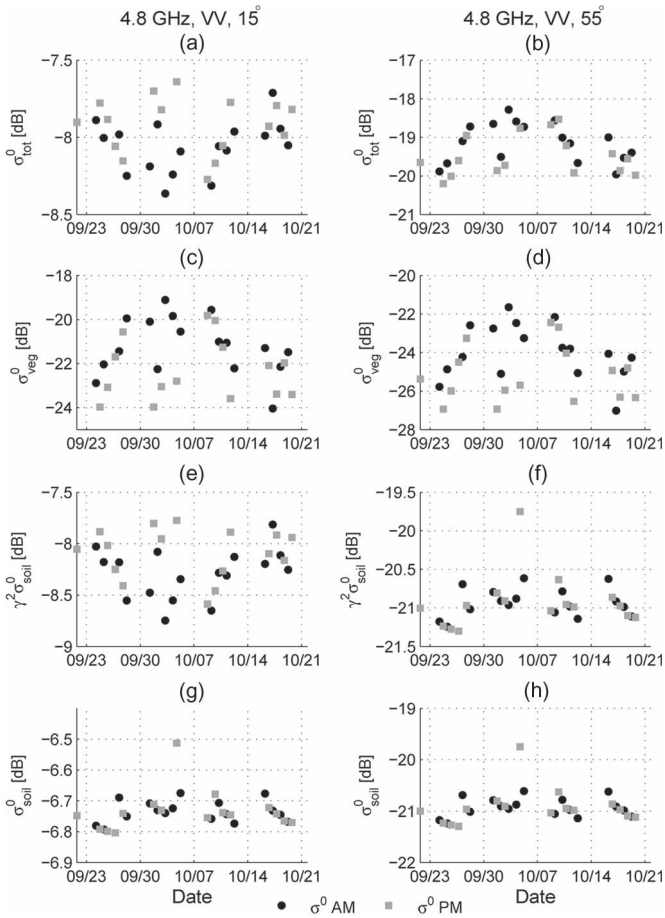

Fig. 11. Modeled radar backscatter time series at vertically polarized C-band (4.8 GHz) using Joseph *et al.* [5]: (a) and (b) total backscatter, (c) and (d) vegetation contribution, (e) and (f) attenuated soil backscatter, and (g) and (h) soil contribution.

significant difference between morning and evening values, it is clear in Fig. 9(b) that the magnitude of the difference is very small.

As mentioned in Section I, diurnal variations in ERS backscatter (also C-band, VV) were observed by Friesen *et al.* [30]. The largest differences coincided with the onset of water stress, when Friesen *et al.* argued that VWC still varies diurnally, but soil moisture is low and does not change significantly. Steele-Dunne *et al.* [32] showed that the diurnal difference observed by Friesen [30] could be explained by variations in leaf moisture content. However, this was for a forest canopy where the VWC is much higher than that considered in Fig. 9.

2) Influence of Incidence Angles at C-Band: Figs. 10 and 11 show the time series of backscatter simulated using (8)–(10) for C-band at different incidence angles and horizontal and vertical polarization, respectively. For both HH and VV polarization, backscatter decreases with increasing incidence angles (-1.2 to -2 dB at 15° and -14 to -20 at 55°). As expected from the sensitivity study, the influence of VWC on backscatter at different incidence angles causes some interesting differences in the diurnal backscatter variations. For all horizontally polarized incidence angles and 15° vertically polarized, a statistically significant diurnal difference was found.

At 15°, the maximum diurnal difference was only 0.4 dB; at 55°, the maximum diurnal difference was 3.5 dB. More interestingly, at 15°, total backscatter was dominated by the attenuated soil backscatter; hence, the drop in VWC during the day results in an increase in backscatter. At 55°, total backscatter is dominated by the direct vegetation contribution and relatively insensitive to soil moisture. In this case, the decrease in VWC during the day leads to a decrease in backscatter.

In general, vertically copolarized backscatter is less than horizontally copolarized backscatter due to the different impact of maize geometry on the two polarizations. Increasing incidence angles still result in a transition to vegetation-dominated total backscatter, but the magnitude of backscatter values and the diurnal differences are smaller than in the horizontally copolarized case. Diurnal differences for both 35° and 55° were not statistically significant.

At C-band, diurnal differences can be attributed to changes in VWC. Close to nadir, it is mainly the attenuation that is affected. At higher angles, VWC mainly influences the vegetation contribution to backscatter, which is the main contribution to total backscatter. These results have some interesting implications. First, this shows that one should be aware of the incidence angle when measuring or combining backscatter data. At different angles, two different mechanisms are influencing

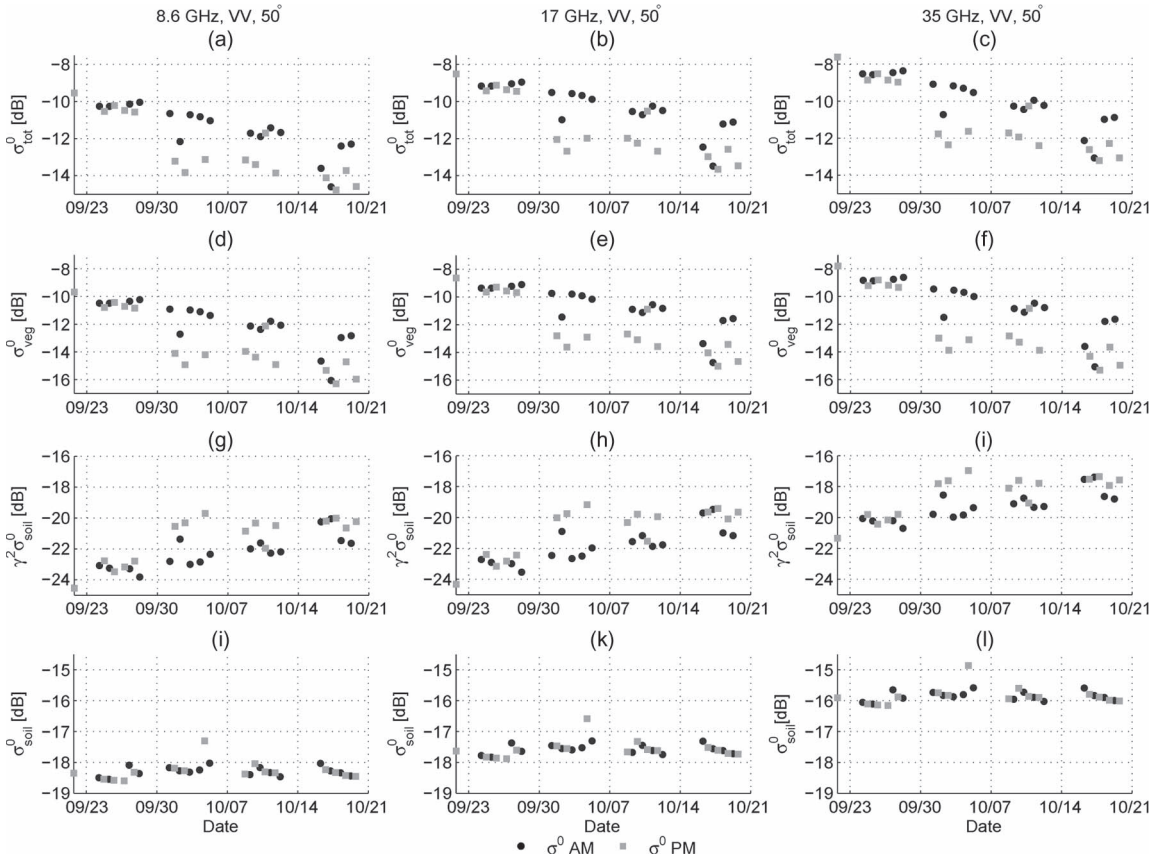

Fig. 12. Modeled time series of vegetation and attenuated soil contributions to total radar backscatter at 8.6, 17, and 35 GHz (VV, 50°) using Ulaby *et al.* [37]: (a)–(c) total backscatter, (d)–(f) vegetation contribution, (g)–(i) attenuated soil backscatter, and (j)–(l) soil contribution.

backscatter (attenuation by vegetation versus direct vegetation backscatter), which might lead to errors in soil moisture retrieval algorithms, if not taken into account properly. Second, results in Fig. 10 show that diurnal variations in C-band (HH) backscatter can be attributed to changes in VWC, which highlights the potential for vegetation and water stress monitoring using radar.

3) High Frequencies: Fig. 12 shows the modeled time series of vegetation and attenuated soil contributions to total backscatter time series for high frequencies (8.6, 17, and 35 GHz) using (9)–(14) and the parameters in [37]. For all frequencies, the direct vegetation contribution is higher than the attenuated soil contribution. As a result, the time series of total backscatter is almost identical to that of the direct vegetation contribution. The magnitude of these terms shift slightly with increasing frequency. The vegetation contribution shifts from a -10 to -17-dB range at 8.6 GHz to a -8 to -15-dB range at 35 GHz. The attenuated soil contribution decreases from a -18 to -25-dB range at 8.6 GHz to a -20 to -27-dB range at 35 GHz. Note that the temporal change in backscatter differs significantly from that shown in Figs. 9 and 10.

In Fig. 12, separate values for leaf and stalk water content were used with (11)–(14). The results in Fig. 11 illustrated that, at high frequencies, total backscatter is mainly influenced by leaf water content. Therefore, the modeled backscatter follows the change in leaf water content, rather than bulk VWC. The decreasing trend in simulated backscatter is caused by the decrease observed in leaf water content. The clear distinction between morning and evening backscatter (up to 4 dB at 35 GHz) between September 30 and October 14, 2012, is due to the observed decrease in leaf VWC during this period. Note that this change in leaf water content is quite small relative to the bulk VWC.

A decrease in VWC can lead to either a decrease or increase in $\sigma^0_{\rm tot}$ depending on the governing contribution to $\sigma^0_{\rm tot}$. At higher frequencies and incidence angles, where the dominant contribution is the signal from vegetation itself, a decrease in VWC during the day leads to a decrease in $\sigma^0_{\rm tot}$. Where the attenuated $\sigma^0_{\rm soil}$ is the main contributor to $\sigma^0_{\rm tot}$, a decrease in VWC leads to an increase in $\sigma^0_{\rm tot}$.

This research shows that even in using vertically copolarized microwaves, the diurnal differences in backscatter can clearly be attributed to changes in VWC. It would be interesting to see how sensitive HH-polarized high-frequency microwaves are to changes in VWC. As shown in Fig. 11, HH-polarized microwaves are more sensitive to changes in VWC. The close correlation between leaf VWC and backscatter highlights the potential of vegetation and water stress monitoring using high-frequency radar.

E. Future Research

Previous research investigated the influence of VWC on $\sigma^0_{\rm tot}$ from the perspective of soil moisture retrieval. Assuming

that VWC changes only on a seasonal scale, vegetation is parameterized. However, given the sensitivity of radar to diurnal differences in VWC, information is lost during this process. This study shows that, for different frequencies, polarizations, and incidence angles, diurnal changes in VWC lead to observable variations in $\sigma^0_{\rm tot}$. During periods of water stress, diurnal differences in radar backscatter can be attributed to vegetation, rather than changes in soil moisture. This sensitivity highlights the use of VWC as a source of information for early water stress detecting in agricultural canopies and to improve vegetation and soil moisture monitoring applications using radar.

Results from this study show that, for a maize canopy, diurnal variation in VWC can be the main influence on total backscatter during periods of low soil moisture variability. Data from this study suggest that VWC dynamics vary in response to water stress. During the day, the amount of water stored in crops (leaves and stalks) decreases by transpiration [48], [49]. As soil moisture decreases, more energy is required for root water uptake [48]. Plants take longer to refill, causing a change in the diurnal cycle of VWC. To fully understand the influence of canopy water dynamics on radar backscatter, more comprehensive experimental data are required.

The observed diurnal difference in VWC (30%–40%) is high and can be attributed to the structure of maize. For other crop types (e.g., alfalfa, beat, sorghum, and soybean), a significant decrease in VWC results in an increase of crop transparency. Consequently, the underlying soil becomes more visible and contributes more to total backscatter. Similar studies with other crops might shed light on the effect of diurnal variation in the VWC of other crops on backscatter.

Detailed *in vivo* data on vegetation and leaf VWC, vegetation dielectric constant, canopy structure, and geometry are needed to improve our understanding of how canopy dynamics influence $\sigma^0_{\rm tot}$. Additional ground-based radar measurements at different frequencies, incidence angles, and polarizations are needed to investigate the significance of fluctuations in VWC in various applications. For example, in soil moisture retrieval and fuel load estimation, diurnal variations and short-term fluctuations in VWC, in response to environmental conditions, are neglected. This may contribute to retrieval errors. Future research will investigate the potential of measuring water stress directly using radar remote sensing.

IV. Conclusion

In this paper, we investigated the diurnal variations in the VWC of a maize canopy and their influence on radar backscatter. Leaf and stalk water content was determined using destructive sampling at 6 A.M. and 6 P.M. over a period of several weeks. A water-cloud model was used to investigate the influence that the observed differences in VWC would have on backscatter at a range of frequencies and angles.

Results from the destructive sampling showed that bulk VWC can vary considerably (up to 1 $\rm kg \cdot m^{-2}$, 30%) between 6 A.M. and 6 P.M., primarily due to changes in stalk VWC. Leaf VWC showed a diurnal difference up to 40 % between morning and evening. Furthermore, leaf VWC decreased with water stress. This was particularly noticeable in the early-morning values.

The sensitivity study using a water-cloud model and bulk VWC demonstrated that, at high frequencies and incidence angles, $\sigma^0_{\rm tot}$ is influenced by variation in both VWC and soil moisture. Fluctuations in VWC have a significant impact on $\sigma^0_{\rm tot}$, particularly when surface soil moisture is dry and fairly constant.

Using a two-layer water-cloud model at high frequencies, it was shown that the simulated difference in $\sigma^0_{\rm tot}$ could be explained by changes in leaf VWC rather than the bulk VWC. Although most of the bulk VWC is in the stalks, fluctuations in the leaf VWC can have a significant impact on radar backscatter.

Statistically significant diurnal differences in backscatter were found for 8.6, 17, and 35 GHz (VV, 50°); 1.275 GHz (VV, 35°); 5.3 GHz (HH, 23°); and 4.8 GHz (HH, 15°–35°; VV, 15°). Morning VWC was statistically significantly higher than evening VWC. When $\sigma^0_{\rm tot}$ is more sensitive to VWC, diurnal variation is caused by direct backscatter from canopy. When soil backscatter is the main contribution, changes in VWC affect the attenuation, leading to diurnal differences in $\sigma^0_{\rm tot}$. During periods of water stress, soil moisture variation is limited, and diurnal differences in $\sigma^0_{\rm tot}$ can be attributed to diurnal variation in VWC.

The results from this study highlight the importance of understanding the mechanisms that control vegetation and leaf water content. A more detailed understanding of leaf water content dynamics and their influence on backscatter may improve soil moisture, biomass, and fuel load retrieval algorithms and shed additional light on how microwave remote sensing could be used to monitor water stress in agricultural canopies.

Acknowledgment

The authors would like to thank the two anonymous reviewers for their constructive feedback, which helped to improve the manuscript significantly.

References

[1] D. Entekhabi *et al.*, "The Soil Moisture Active Passive (SMAP) mission," *Proc. IEEE*, vol. 98, no. 5, pp. 704–716, May 2010.

[2] P. C. Dubois, J. van Zyl, and T. Engman, "Measuring soil moisture with imaging radars," *IEEE Trans. Geosci. Remote Sens.*, vol. 33, no. 4, pp. 915–926, Jul. 1995.

[3] Y. Kim and J. J. van Zyl, "A time-series approach to estimate soil moisture using polarimetric radar data," *IEEE Trans. Geosci. Remote Sens.*, vol. 47, no. 8, pp. 2519–2527, Aug. 2009.

[4] A. Joseph, R. van der Velde, P. O'Neill, and R. Lang, "Soil moisture retrieval during a corn growth cycle using L-band (1.6 GHz) radar observations," *IEEE Trans. Geosci. Remote Sens.*, vol. 46, no. 8, pp. 2365–2374, Aug. 2008.

[5] A. Joseph, R. van der Velde, P. O'Neill, R. Lang, and T. Gish, "Effects of corn on C- and L-band radar backscatter: A correction method for soil moisture retrieval," *Remote Sens. Environ.*, vol. 114, no. 11, pp. 2417–2430, Nov. 2010.

[6] R. Bindlish and A. Barros, "Parameterization of vegetation backscatter in radar-based soil moisture estimation," *Remote Sens. Environ.*, vol. 76, no. 1, pp. 130–137, Apr. 2001.

[7] G. M. Foody, P. Curran, G. Groom, and D. Munro, "Multi-temporal airborne synthetic aperture radar data for crop 468 classification," *Geocarto Int.*, vol. 4, no. 3, pp. 19–29, 1989.

[8] H. McNairn, J. Shang, X. Jiao, and C. Champagne, "The contribution of ALOS PALSAR multipolarization and polarimetric data to crop classification," *IEEE Trans. Geosci. Remote Sens.*, vol. 47, no. 12, pp. 3981–3992, Dec. 2009.
[9] F. T. Ulaby, R. Y. Li, and K. Shanmugan, "Crop classification using airborne radar and Landsat data," *IEEE Trans. Geosci. Remote Sens.*, vol. GE-20, no. 1, pp. 42–51, Jan. 1982.
[10] P. Hoogeboom, "Classification of agricultural crops in radar images," *IEEE Trans. Geosci. Remote Sens.*, vol. GE-21, no. 3, pp. 329–336, Jul. 1983.
[11] S. Paloscia, G. Macelloni, P. Pampaloni, and S. Sigismondi, "The potential of C- and L-band SAR in estimating vegetation biomass: The ERS-1 and JERS-1 experiments," *IEEE Trans. Geosci. Remote Sens.*, vol. 37, no. 4, pp. 2107–2110, Jul. 1999.
[12] P. Ferrazzoli *et al.*, "The potential of multifrequency polarimetric SAR in assessing agricultural and arboreous biomass," *IEEE Trans. Geosci. Remote Sens.*, vol. 35, no. 1, pp. 5–17, Jan. 1997.
[13] J. Q. Chambers *et al.*, "Regional ecosystem structure and function: Ecological insights from remote sensing of tropical forests," *Trends Ecol. Evol.*, vol. 22, no. 8, pp. 414–423, Aug. 2007.
[14] S. Saatchi, K. Halligan, D. G. Despain, and R. L. Crabtree, "Estimation of forest fuel load from radar remote sensing," *IEEE Trans. Geosci. Remote Sens.*, vol. 45, no. 6, pp. 1726–1740, Jun. 2007.
[15] P. E. O'Neill, E. Podest, and E. G. Njoku, "Utilization of ancillary data sets for SMAP algorithm development and product generation," in *Proc. IEEE IGARSS*, 2011, pp. 2436–2439.
[16] H. McNairn and B. Brisco, "The application of C-band polarimetric SAR for agriculture: A review," *Can. J. Remote Sens.*, vol. 30, no. 3, pp. 525–542, Jan. 2004.
[17] R. Bindlish *et al.*, "Combined passive and active microwave observations of soil moisture during CLASIC," *IEEE Geosci. Remote Sens. Lett.*, vol. 6, no. 4, pp. 644–648, Oct. 2009.
[18] R. Panciera *et al.*, "The Soil Moisture Active Passive Experiments (SMAPEx): Towards soil moisture retrieval from the SMAP mission," *IEEE Trans. Geosci. Remote Sens.*, vol. 52, no. 1, pp. 490–507, Jan. 2014.
[19] S. Kim, J. van Zyl, K. McDonald, and E. Njoku, "Monitoring surface soil moisture and freeze-thaw state with the high-resolution radar of the Soil Moisture Active/Passive (SMAP) mission," in *Proc. IEEE Radar Conf.*, 2010, pp. 735–739.
[20] W. Wagner, G. Lemoine, and H. Rott, "A method for estimating soil moisture from ERS scatterometer and soil data," *Remote Sens. Environ.*, vol. 70, no. 2, pp. 191–207, Nov. 1999.
[21] V. Naeimi, Z. Bartalis, and W. Wagner, "ASCAT soil moisture: An assessment of the data quality and consistency with the ERS scatterometer heritage," *J. Hydrometeorol.*, vol. 10, no. 2, pp. 191–207, Nov. 2009.
[22] I. Birrer, E. Bracalente, G. Dome, J. Sweet, and G. Berthold, "σ signature of the Amazon rain forest obtained from the SeaSat scatterometer," *IEEE Trans. Geosci. Remote Sens.*, vol. GE-20, no. 1, pp. 11–17, Jan. 1982.
[23] M. Satake and H. Hanado, "Diurnal change of Amazon rain forest σ_0 observed by Ku-band spaceborne radar," *IEEE Trans. Geosci. Remote Sens.*, vol. 42, no. 6, pp. 1127–1134, Jun. 2004.
[24] F. T. Ulaby and P. P. Batlivala, "Optimum radar parameters for mapping soil moisture," *IEEE Trans. Geosci. Electron.*, vol. GE-14, no. 2, pp. 81–93, Apr. 1976.
[25] B. Brisco, R. Brown, J. Koehler, G. Sofko, and M. McKibben, "The diurnal pattern of microwave backscattering by wheat," *Remote Sens. Environ.*, vol. 34, no. 1, pp. 37–47, Oct. 1990.
[26] K. McDonald, M. Dobson, and F. Ulaby, "Using MIMICS to model L-band multiangle and multitemporal backscatter from a walnut orchard," *IEEE Trans. Geosci. Remote Sens.*, vol. 28, no. 4, pp. 477–491, Jul. 1990.
[27] S. Frolking *et al.*, "Tropical forest backscatter anomaly evident 510 in SeaWinds scatterometer morning overpass data during 2005 drought in Amazonia," *Remote Sens. Environ.*, vol. 115, no. 3, pp. 897–907, Mar. 2011.
[28] S. Jaruwatanadilok and B. W. Stiles, "Trends and variation in Ku-band backscatter of natural targets on land observed in QuikSCAT data," *IEEE Trans. Geosci. Remote Sens.*, vol. 52, no. 7, pp. 4838–4390, Jul. 2014.
[29] J. Friesen, "Regional vegetation water effects on satellite soil moisture estimations for West Africa," in *Ecology and Development Series*, no. 63, Bonn, Germany: Zentrum für Entwicklungsforschung (ZRF), 2008.
[30] J. Friesen *et al.*, "Spatial and seasonal patterns of diurnal differences in ERS scatterometer soil moisture data in the Volta Basin, West Africa," in *IAHS Red Book Series*, vol. 316. Wallingford, U.K.: IAHS Press, 2007, pp. 47–55.
[31] J. Friesen, S. C. Steele-Dunne, and N. van de Giesen, "Diurnal differences in global ERS scatterometer backscatter observations of the land surface," *IEEE Trans. Geosci. Remote Sens.*, vol. 50, no. 7, pp. 2595–2602, Jul. 2012.
[32] S. C. Steele-Dunne, J. Friesen, and N. van de Giesen, "Using diurnal variation in backscatter to detect vegetation water stress," *IEEE Trans. Geosci. Remote Sens.*, vol. 50, no. 7, pp. 2618–2629, Jul. 2012.
[33] F. Ulaby, K. Sarabandi, K. McDonald, M. Whitt, and C. Dobson, "Michigan microwave canopy scattering model," *Int. J. Remote Sens.*, vol. 11, no. 7, pp. 1223–1253, Jul. 1990.
[34] E. Attema and F. Ulaby, "Vegetation modeled as a water cloud," *Radio Sci.*, vol. 13, no. 2, pp. 357–364, Mar./Apr. 1978.
[35] L. J. Abendroth, R. Elmore, M. Boyer, and S. Marlay, *Corn Growth and Development. PMR 1009*. Ames, AI, USA: Iowa State University Extension, 2011.
[36] R. G. Allen, L. Pereira, D. Raes, and M. Smith, *FAO Irrigation and Drainage Paper No. 56*. Quebec, QC, Canada: Food and Agriculture Organization of the United Nations, 1998, pp. 26–40.
[37] F. Ulaby, C. Allen, G. Eger, and E. Kanemasu, "Relating the microwave backscattering coefficient to leaf area index," *Remote Sens. Environ.*, vol. 14, no. 1–3, pp. 113–133, Jan. 1984.
[38] K. Dabrowska-Zielinksa, Y. Inoue, W. Kowalik, and M. Gruszcynska, "Inferring the effect of plant and soil variables on C- and L-band SAR backscatter over agricultural fields, based on model analysis," *Adv. Space Res.*, vol. 39, no. 1, pp. 139–148, 2007.
[39] L. Prévot, I. Champion, and G. Guyot, "Estimating surface soil moisture and leaf area index of a wheat canopy using a dual-frequency (C and X bands) scatterometer," *Remote Sens. Environ.*, vol. 46, no. 3, pp. 331–339, Dec. 1993.
[40] I. Champion, L. Prevot, and G. Guyot, "Generalized semi-empirical modelling of wheat radar response," *Int. J. Remote Sens.*, vol. 21, no. 9, pp. 1945–1951, Jan. 2000.
[41] Y. Oh and K. Sarabandi, "An empirical model and an inversion technique for radar scattering from bare soil surfaces," *IEEE Trans. Geosci. Remote Sens.*, vol. 30, no. 2, pp. 370–311, Mar. 1992.
[42] Y. Oh, "Quantitative retrieval of soil moisture content and surface roughness from multipolarized radar observations of bare soil surfaces," *IEEE Trans. Geosci. Remote Sens.*, vol. 42, no. 3, pp. 596–601, Mar. 2004.
[43] M. C. Dobson and F. T. Ulaby, "Active microwave soil moisture research," *IEEE Trans. Geosci. Remote Sens.*, vol. GE-24, no. 1, pp. 23–36, Jan. 1986.
[44] M. T. van Genuchten and D. R. Nielsen, "On describing and predicting the hydraulic properties of unsaturated soils," *Ann. Geophys.*, vol. 3, no. 5, pp. 615–628, 1985.
[45] J. Simunek and M. van Genuchten, "Estimating unsaturated soil hydraulic properties from tension disc infiltrometer data by numerical inversion," *Water Resour. Res.*, vol. 32, no. 9, pp. 2683–2696, Apr. 1996.
[46] F. T. Ulaby, R. K. Moore, and A. K. Fung, *Microwave Remote Sensing, Active and Passive, II, Radar Remote Sensing and Surface Scattering and Emission Theory*. Norwood, MA, USA: Artech House, 1982.
[47] T. Jackson and T. Schmugge, "Vegetation effects on the microwave emission of soils," *Remote Sens. Environ.*, vol. 36, no. 3, pp. 203–212, Jun. 1991.
[48] R. Slayter, *Plant-Water Relationships*. London, U.K.: Academic, 1967.
[49] W. Larcher, *Physiological Plant Ecology*. Berlin, Germany: Springer-Verlag, 1995.

Tim van Emmerik (S'14) received the B.Sc. and M.Sc. degrees in civil engineering from the Delft University of Technology, Delft, The Netherlands, in 2011 and 2013, respectively. He is currently working toward the Ph.D. degree with the Water Resources Section, Faculty of Civil Engineering and Geosciences, Delft University of Technology, where the topic of his thesis is understanding the effect of vegetation on radar backscatter for water stress detection in agricultural crops.

Mr. van Emmerik is the 2014 and 2015 AGU Hydrology Section Student Representative and is a cofounder of the Young Hydrologic Society, a bottom-up organization that aims to represent, connect, and involve early career scientists in the hydrologic community. He is a Student Member of the American Geophysical Union and the European Geosciences Union.

Susan C. Steele-Dunne received the S.M. and Ph.D. degrees in hydrology from the Massachusetts Institute of Technology, Cambridge, MA, USA, in 2002 and 2006, respectively.

Since 2008, she has been with the Water Resources Section, Faculty of Civil Engineering and Geosciences, Delft University of Technology, Delft, The Netherlands. Her research interests include remote sensing, data assimilation, land–atmosphere interactions, and land surface modeling.

Dr. Steele-Dunne is a member of the American Meteorological Society and the American Geophysical Union. She has also served the American Geophysical Union Hydrology Section as a member of the Remote Sensing Technical Committee and the Hydrological Sciences Award committee, and the American Meteorological Society as a member of the Hydrology Committee.

Jasmeet Judge (S'94–M'00–SM'05) received the Ph.D. degree in electrical engineering and atmospheric, oceanic, and space sciences from the University of Michigan, Ann Arbor, MI, USA, in 1999.

She is currently an Associate Professor with the Department of Agricultural and Biological Engineering, Institute of Food and Agricultural Sciences, University of Florida, Gainesville, FL, USA, where she is also the Director of the Center for Remote Sensing. Her research interests are in microwave remote sensing applications to terrestrial hydrology for dynamic vegetation; modeling of energy and moisture interactions at the land surface and in the vadose zone; spatial and temporal scaling of remotely sensed observations in heterogeneous landscapes; and data assimilation.

Dr. Judge is the Chair of the National Academies' Committee on Radio Frequencies and a member of the Frequency Allocations in Remote Sensing Technical Committee in the IEEE-GRSS. She also serves the American Geophysical Union as the past Chair of the Remote Sensing Technical Committee in the Hydrology Section.

Nick van de Giesen received the B.S. (*Kandidaats*) degree and the M.Sc. degree in land and water management from the Wageningen Agricultural University, Wageningen, The Netherlands, in 1984 and 1987, respectively, and the Ph.D. degree in agricultural and biological engineering from Cornell University, Ithaca, NY, USA, in 1994.

After a postdoctoral position with the West Africa Rice Development Association, Bouak, Côte d'Ivoire, he was a Senior Researcher for six years with the Center for Development Research (ZEF), University of Bonn, Bonn, Germany, where he was the Scientific Coordinator of the Global Change in the Hydrological Cycle Volta Project. Since 2004, he has been with the Water Resources Section, Faculty of Civil Engineering and Geosciences, Delft University of Technology, Delft, The Netherlands, where he currently holds the van Kuffeler Chair of Water Resources Management.

Dr. van de Giesen is a cofounder of the Trans-African Hydro-Meteorological Observatory; a member of scientific advisory boards in Germany, Finland, and The Netherlands; and a recipient of the 2015 Darcy Medal of the European Geosciences Union. He is also a Senior Fellow of the ZEF.